厚生労働科学研究費補助金
医療機器開発推進研究事業

循環腫瘍細胞観察可能なナノ粒子質量顕微鏡開発に関する研究

平成24年度　総括研究報告書

研究代表者　瀬藤　光利

平成25（2013）年4月

目　　次

厚生労働科学研究費補助金（医療機器開発推進研究事業）　総括研究報告書

循環腫瘍細胞観察可能なナノ粒子質量顕微鏡開発に関する研究

研究代表者　浜松医科大学・解剖学講座・細胞生物学分野　教授　瀬藤光利

研究要旨

癌が進展するごく早期から血中に存在する循環腫瘍細胞の質的評価は診断・治療に重要である。本研究は、研究代表者が開発した質量顕微鏡装置を用いて循環腫瘍細胞の質的評価を行うことを目的とする。本事業年度は乳癌患者末梢血から循環腫瘍細胞を精製・回収し、脂質化合物に着目した一細胞質量顕微鏡解析を行い、網羅的データ解析に供した。ナノ粒子付与基盤の評価を行い、検討結果を基に一細胞質量顕微鏡のための新規素材を創出した。本研究で樹立した一細胞質量顕微鏡法による循環腫瘍細胞の質的評価系を臨床検体に応用した。

研究分担者氏名・所属研究機関名及び所属研究機関における職名

瀬藤光利　浜松医科大学・解剖学講座・細胞生物学分野　教授

池上浩司　浜松医科大学・解剖学講座・細胞生物学分野　准教授

早坂孝宏　浜松医科大学・解剖学講座・細胞生物学分野　特任助教

A．研究目的

厚生労働行政において癌対策及び癌研究の推進は重要な位置を占める。癌の早期診断、予後判定、治療効果判定はいずれも重要な課題であり、その方法が種々議論され開発されてきた。転移に関する分子メカニズムの解明は、これらいずれの課題にも極めて重要な解決の糸口となりうるテーマである。転移に関して提唱され注目を集めている新規モデルは、従来考えられてきたよりもごく早い病期のうちから、癌細胞が血液中に流れ出し、やがて多臓器に生着し転移巣を形成するというものである。この血液中に存在する腫瘍細胞は循環腫瘍細胞と呼ばれ、検出個数と予後の悪さには正の相関関係があることが知られている。一方で循環腫瘍細胞の質的な評価に関しては細胞表面マーカーや遺伝子発現に着目した報告が行われているのみであり、評価方法は未だ十分に確立されていない。本研究はこの評価方法を提唱するために循環腫瘍細胞の収集と解析を行うことを目的とする。

本研究では、質量顕微鏡法による腫瘍組織および循環腫瘍細胞の解析を行い、その生物学的特性を明らかにして腫瘍細胞機能イメージング新評価システムを確立し、病理検査に応用する。質量顕微鏡法は研究代表者らが開発してきた質量分析手法であり、生体試料を直接的に二次元質量分析することにより、試料組織上生体物質の種類、位置、相対量を解析する手法である。本研究では、新たな循環腫瘍細胞の質的評価方法の確立を目指すために、担癌患者検体から循環腫瘍細胞を回収しナノ粒子質量顕微鏡法による統合的解析を行うことを目的とする。末梢血および参照試料としての原発巣組織の採取対象として乳癌を設定した。乳癌は女性特有の癌であり、中年齢層における発症が少なくないことから、本研究は厚生労働行政の目指す「女性特有のがん対策の推進」及び「働く世代のがん対策」に貢献すると考えられる。

本事業年度は、臨床検体からの循環腫瘍細胞回収と質量顕微鏡観察実施のため、1) 担癌患者検体の収集、2) 担癌患者より採取した末梢血から循環腫瘍細胞を回収する手法の最適化、3) 一細胞ナノ粒子質量顕微鏡解析法の最適化、4) 臨床検体の一細胞質量顕微鏡解析を行った。

B．研究方法

1) 臨床検体の取得にあたっては、浜松医科大学乳腺外科で診断もしくは治療を目的として組織採取を行う乳癌患者を対象とした。十分なインフォームドコンセントの後、同意の得られた患者から、生検組織採取とともに循環腫瘍細胞採取のため末梢血の採血を行った。収集検体の背景情報は、研究協力者の所属施設において連結可能匿名化の上管理した。

2) 循環腫瘍細胞の選択の基本手法としては、全体計画の通り磁気細胞分離法とフローサイトメトリー法を利用した。正常人血液に細胞株を添加し作製するモデル血液での実験には、乳癌細胞株 SKBR-3 を培養し用いた。遠沈管による処理、及び細胞選別のための抗体クローンにつき最適化を行った。

3) 細胞及び組織の回収・質量顕微鏡解析条件を、接着状態と質量顕微鏡解析におけるシグナル強度に基づき比較検討した。銀、金、インジウム酸化スズ粒子を付与したスライドグラスを用いた。質量顕微鏡解析の条件としてレーザーエネルギー、空間解像度、測定領域範囲、測定質量範囲等を最適化した。

4) 原発巣の単一細胞化には、研究全体計画時に考

案した通り、検体組織をメスで小断片化した後に酵素処理する方法を用いた。フローサイトメトリー法により細胞を回収し、一細胞質量顕微鏡解析した。

（倫理面への配慮）

本研究は浜松医科大学の医の倫理審査委員会による承認を受けた。該当する患者に当研究に関して患者用説明文書を用い、研究への協力の可否が治療の質に影響しないこと、研究への協力が危険を伴わないこと、研究協力者及び家族の意思を第一に尊重することを十分に説明し、インフォームドコンセントを得られた場合、文書による同意書を得て、疫学研究に関する倫理指針（平成１６年文部科学省・厚生労働省告示第２号）および臨床研究に関する倫理指針（平成１６年厚生労働省告示第４５９号）に厳正に則り研究を施行した。試料は連結可能匿名化を行い情報管理者が適切に管理した。

C．研究結果

1) 初年度に引き続き平成 24 年度も継続して検体の収集を行うとした全体研究計画の通り、乳癌臨床検体につき末梢血・原発巣組織の収集と循環腫瘍細胞・原発巣腫瘍細胞の精製・解析を行った。検体番号 20 から 50 までの 31 回の測定において、患者末梢血 12.5 ml 中に循環腫瘍細胞が 1 個検出される事例を 5 例得た。

2) 乳癌細胞株を用い循環腫瘍細胞の精製条件を最適化した。新規遠沈管の導入により処理時間を短縮することができた。

3) 銀、金、インジウム酸化スズ粒子の付与によりシグナル強度上昇が見られるかどうかを、一細胞質量顕微鏡解析により調べた。金薄膜付与基盤あるいはインジウム酸化スズ付与スライドグラスを比較対照とした実験において、有意差を持ってシグナル強度の向上を示す分子は見いだされなかった。一方、インジウム酸化スズ付与スライドグラスに特殊コーティングを施すことにより、シグナル強度は保持したまま試料接着性を向上できることが判明した。一細胞質量顕微鏡解析にも本素材は有用であり、製品化を進めた。

4) 一部の検体を用い CD326 陽性、CD45 陰性細胞（循環腫瘍細胞に相当）の質量顕微鏡解析を行った。新規解析ソフトウェアを導入し、原発巣検体試料に由来する細胞の質量顕微鏡法解析結果との比較を行ったところ、循環腫瘍細胞相当の細胞集団が原発巣由来の細胞集団に比べ低いシグナル強度を示す分子を複数見出すことができた。また、測定領域内でのシグナル強度のばらつきを標準偏差で評価することにも成功した。本測定実施後に循環腫瘍細胞の定義領域を、バックグラウンドノイズのより少ないものへと変更したため、本結果の妥当性につき検体数を増やし確認中である。

D．考察

1) 症例の収集に際し臨床医と連携することで、予定を上回るペースで検体の収集を行うことができた。他施設との連携も実現できたため、最終年度はデータ解析に供する検体数を増やし更なる数の循環腫瘍細胞の分子プロファイルを取得し、臨床情報と質量顕微鏡解析結果の統合的解析を行う予定である。

2) 循環腫瘍細胞の選択・回収手法確立においては、安定した水準で回収ができる条件が整ったと考える。モデル血液を用いた複数回の施行において、常時約 40%の回収率で循環腫瘍細胞を検出・回収できることを確認済みである。

3) 基盤の比較検討から、一細胞質量顕微鏡法解析に適した新たな素材として特殊コーティングスライドグラスが創出された。本素材を解析に利用することで細胞接着と希少試料取得の効率向上が期待される。

4) 循環腫瘍細胞の性状解析に関する研究として本年度は他研究機関より膵癌の循環腫瘍細胞のマイクロアレイ解析の研究結果が報告されたが、脂質解析については未だ報告は寄せられていない。本研究で臨床検体を用い進めている質量顕微鏡解析では脂質分子を始めとする低分子代謝物が検出されており、原発巣細胞との組成比較手法も確立済みである。我々は独自の基軸による循環腫瘍細胞の性状評価を実現しつつある。

E．結論

乳癌患者臨床検体を用いた循環腫瘍細胞の精製・回収を施行し、質量顕微鏡法解析を行った。ソフトウェア解析により低分子代謝物を網羅解析することを可能とし、本手法を一部の臨床検体試料に適用することで、原発巣由来細胞と循環腫瘍細胞の間で異なる検出傾向を示す分子群を見出した。ナノ粒子を利用した一細胞質量顕微鏡法解析の手法確立の過程から新規素材を創出することができた。

F．健康危険情報

本事業年度は特に健康危険情報は報告すべきものはなかった。

G．研究発表

1. 論文発表

【原著論文】

(1) Ishikawa S, Tateya I, Hayasaka T, Masaki N, Takizawa Y, Ohno S, Kojima T, Kitani Y, Kitamura M, Hirano S, Setou M, Ito J. Increased expression of phosphatidylcholine (16:0/18:1) and (16:0/18:2) in thyroid papillary

cancer. PloS One 2012;7(11):e48873.

【英文総説】

(1) Nakanishi T, Setou M, Kuhara T. Biomedical mass spectrometry. Anal Bioanal Chem. 2012 Jun;403(7):1775-6. doi: 10.1007/s00216-012-5922-x. No abstract available.
(2) Saito Y, Waki M, Hammed S, Hayasaka T, Setou M. Development of Imaging Mass Spectrometry. Biol Pharm Bull. 2012 Sep;35(9):1417-24.
(3) Goto K, Waki M, Takahashi T, Kadowaki M, Setou M. High-Resolution Multi-isotope Imaging Mass Spectrometry Enables Visualisation of Stem Cell Division and Metabolism. ChemBioChem. 2012 May 29;13(8):1103-6. Epub 2012 Apr 19.

【英文著書】

(1) Sugiura Y, Yao I, Setou M. Imaging mass spectrometry (IMS) for biological application. MASS SPECTROMETRY HANDBOOK 2012;41-83.
(2) Shrivas K, Setou M. Imaging Mass Spectrometry: Sample Preparation, Instrumentation, and Applications. Advances in IMAGING and ELECTRON PHYSICS. 2012;171:145-193.

【和文総説】

(1) 門脇慎、稲見勝朗、脇紀彦、高橋司、後藤健介、瀬藤光利 医学・薬学分野における質量顕微鏡法の利用 医薬ジャーナル 8 月号、2012 年 48 巻 8 号 p2011-2014
(2) 後藤健介、高橋司、脇紀彦、瀬藤光利 (展望) 質量顕微鏡法の展望 ぶんせき、2012 年 9 号 p495-498
(3) 瀬藤光利 質量顕微鏡：電子顕微鏡との接点 医学生物学電子顕微鏡技術学会誌、2012 年 26 巻 1 号 p39-40
(4) 瀬藤光利 質量顕微鏡法 YAKUGAKU ZASSI、2012 年 4 月 132 巻 4 号 p499-506

【和文著書】

(1) 早坂孝宏、瀬藤光利 現代質量分析学 基礎原理から応用研究まで イメージング 化学同人、2013 年 1 月 15 日 p345-357

2. 学会発表

(1)瀬藤光利、Imaging mass spectrometry of Sphingolipids、EMBO Workshop on Molecular Medicine of Sphingolipids、イスラエル、2012 年 10 月

(2)脇紀彦、井手佳美、高橋司、後藤健介、古川省悟、高橋郁太、佐藤哲朗、白井祐輔、門脇慎、稲見勝朗、大畑健次、椎谷紀彦 、瀬藤光利、乳癌循環腫瘍細胞のフローサイトメトリー法による精製と質量顕微鏡法による解析、第 22 回日本サイトメトリー学会学術集会、大阪、2012 年 6 月

H. 知的財産権の出願・登録状況

1. 特許取得

(1)出願番号：2012-102636 出願日：2012/4/27
タイトル：質量分析データ処理方法及び装置、発明人：松浦正明、牛嶋大、涌井昌俊、瀬藤光利、梶原茂樹、小河潔
(2)出願番号：2013-018659、出願日：2013/2/1
タイトル：乳癌治療剤の有効性評価方法及び被験者選択方法、発明人：瀬藤光利、井手佳美、脇紀彦

研究成果の刊行に関する一覧表

雑誌【原著論文】

発表者氏名	論文タイトル名	発表誌名	巻号	ページ	出版年
Ishikawa S, Tateya I, Hayasaka T, Masaki N, Takizawa Y, Ohno S, Kojima T, Kitani Y, Kitamura M, Hirano S, Setou M, Ito J.	Increased Expression of Phosphatidylcholine (16:0/18:1) and (16:0/18:2) in Thyroid Papillary Cancer	PloS One	7(11)	e48873	2012 Nov

雑誌【英文総説】

発表者氏名	論文タイトル名	発表誌名	巻号	ページ	出版年
Nakanishi T, Setou M, Kuhara T.	Biomedical mass spectrometry.	Anal Bioanal Chem.	403(7)	1775-6	2012
Saito Y, Waki M, Hammed S, Hayasaka T, Setou M.	Development of Imaging Mass Spectrometry.	Biol Pharm Bull.	35(9)	1417-24	2012
Goto K, Waki M, Takahashi T, Kadowaki M, Setou M.	High-Resolution Multi-isotope Imaging Mass Spectrometry Enables Visualisation of Stem Cell Division and Metabolism.	ChemBioChem.	13(8)	1103-6	2012

書籍【英文著書】

著者氏名	論文タイトル名	書籍全体の編集者名	書　籍　名	出版社名	出版地	出版年	ページ
Sugiura Y, Yao I, Setou M.	Imaging mass spectrometry (IMS) for biological application.	MIKE S.LEE	MASS SPECTROMETRY HANDBOOK	WILEY	USA	2012	41-83
Shrivas K, Setou M.	Imaging Mass Spectrometry: Sample Preparation, Instrumentation, and Applications.	PETER W. HAWKES	Advances in IMAGING and ELECTRON PHYSICS.	ACADEMIC PRESS	USA	2012	145-193

雑誌【和文総説】

発表者氏名	論文タイトル名	発表誌名	巻号	ページ	出版年
門脇慎、稲見勝朗、脇紀彦、高橋司、後藤健介、瀬藤光利	医学・薬学分野における質量顕微鏡法の利用	医薬ジャーナル	48巻8号	p2011-2014	2012年
後藤健介、高橋司、脇紀彦、瀬藤光利	展望）質量顕微鏡法の展望	ぶんせき	9号	p495-498	2012年
瀬藤光利	質量顕微鏡：電子顕微鏡との接点	医学生物学電子顕微鏡技術学会誌	26巻1号	p39-40	2012年
瀬藤光利	質量顕微鏡法	YAKUGAKU ZASSI	132巻4号	p499-506	2012年

書籍　【和文著書】

著者氏名	論文タイトル名	書籍全体の編集者名	書　籍　名	出版社名	出版地	出版年	ページ
早坂孝宏、瀬藤光利	イメージング	高山光男、早川滋雄、瀧浪欣彦、和田芳直	現代質量分析学　基礎原理から応用研究まで	化学同人	日本	2013年	p345-357

研究成果の刊行物

次頁参照

OPEN ACCESS Freely available online

PLOS | ONE

Increased Expression of Phosphatidylcholine (16:0/18:1) and (16:0/18:2) in Thyroid Papillary Cancer

Seiji Ishikawa[1], Ichiro Tateya[1]*, Takahiro Hayasaka[2], Noritaka Masaki[2], Yoshinori Takizawa[3], Satoshi Ohno[1], Tsuyoshi Kojima[1], Yoshiharu Kitani[1], Morimasa Kitamura[1], Shigeru Hirano[1], Mitsutoshi Setou[2], Juichi Ito[1]

1 Department of Otolaryngology-Head and Neck Surgery, Graduate School of Medicine, Kyoto University, Kyoto, Japan, **2** Department of Cell Biology and Anatomy, Hamamatsu University School of Medicine, Hamamatsu, Japan, **3** Department of Otolaryngology/Head and Neck Surgery, Hamamatsu University School of Medicine, Hamamatsu, Japan

Abstract

A good prognosis can be expected for most, but not all, cases of thyroid papillary cancer. Numerous molecular studies have demonstrated beneficial treatment and prognostic factors in various molecular markers. Whereas most previous reports have focused on genomics and proteomics, few have focused on lipidomics. With the advent of mass spectrometry (MS), it has become possible to identify many types of molecules, and this analytical tool has become critical in the field of omics. Recently, imaging mass spectrometry (IMS) was developed. After a simple pretreatment process, IMS can be used to examine tissue sections on glass slides with location information. Here, we conducted an IMS analysis of seven cases of thyroid papillary cancer by comparison of cancerous with normal tissues, focusing on the distribution of phospholipids. We identified that phosphatidylcholine (16:0/18:1) and (16:0/18:2) and sphingomyelin (d18:0/16:1) are significantly higher in thyroid papillary cancer than in normal thyroid tissue as determined by tandem mass (MS/MS) analysis. These distributional differences may be associated with the biological behavior of thyroid papillary cancer.

Citation: Ishikawa S, Tateya I, Hayasaka T, Masaki N, Takizawa Y, et al. (2012) Increased Expression of Phosphatidylcholine (16:0/18:1) and (16:0/18:2) in Thyroid Papillary Cancer. PLoS ONE 7(11): e48873. doi:10.1371/journal.pone.0048873

Editor: Yunli Zhou, Harvard Medical School, United States of America

Received May 18, 2012; **Accepted** October 2, 2012; **Published** November 6, 2012

Funding: This study was supported by a SENTAN grant from the Japan Science and Technology Agency to MS (http://www.jst.go.jp/sentan/en/); a Grant-in-Aid for Scientific Research to MS (WAKATE-S: 20670004, http://www.jsps.go.jp); and a grant from the Ministry of Education, Culture, Sports, Science and Technology, Japan to IT and MK. The funders had no role in study design, data collection and analysis, decision to publish, or preparation of the manuscript.

Competing Interests: The authors have declared that no competing interests exist.

* E-mail: tateya@ent.kuhp.kyoto-u.ac.jp

Introduction

Thyroid cancer is the most common malignant tumor in the head and neck region. The histological types of thyroid cancer vary, and include papillary carcinoma (80% of all thyroid cancer cases), follicular carcinoma, medullary carcinoma, and undifferentiated carcinoma. Prognosis also varies depending on histological type. Undifferentiated carcinoma has a poor prognosis, with a 10-year survival rate of 10–20% or less, whereas patients with other histological types, such as papillary carcinoma, follicular carcinoma, and medullary carcinoma, can expect good outcomes with a 10-year survival rate of 90%, 90%, and 70–80%, respectively [1]. However, even cases of papillary carcinoma can fail to be controlled due to distant metastasis or anaplastic transformation. It will be necessary to reliably predict anaplastic transformation before it occurs, and to identify cases of poor prognosis among papillary carcinomas, in order to improve the overall prognosis of thyroid cancer.

Developments in genomics and molecular biology have shed light on pathogenic mechanisms related to thyroid cancer [2]. Great efforts have been made to identify genes and biomolecules that are differentially expressed in cancerous tissues, which can be utilized as biomarkers to elucidate thyroid cancer pathogenesis and guide appropriate and targeted molecular therapies [3,4,5]. Several candidate genes (for TSH receptors, RET/PTC, Ras, BRAF, p53) in the development of different types of thyroid cancer [2] have been identified thus far. In addition, some attempts have been made to utilize proteomics as a tool of discovery for thyroid neoplasms. Lewis and co-workers reported a difference in protein expression between papillary thyroid carcinoma and normal thyroid tissue using mass spectrometry (MS) [6]. However, the mechanism of malignant transformation is not well understood, especially at the protein level.

Lipids are associated with cell membrane structure, proliferation [7], differentiation, metabolic regulation, inflammation [8], and immunity. It is important to understand the relationship between tumor and lipids in diagnosis and treatment. Lipids, especially phospholipids (PLs), play important roles in the composition of the cell membrane. It is generally accepted that membrane characteristics are determined by the components of PL species, and the composition of these species is strictly determined by the components of fatty acid species [9,10]. A few reports conducted to date have focused on lipids, especially binding fatty acids in head and neck cancer; however, to date, no method has been developed that enables the detection of binding fatty acids in PLs.

Imaging mass spectrometry (IMS) is a powerful, newly developed tool that identifies the distribution of known/unknown molecules on a tissue section [11,12,13]. Laser scanning enables precise, two-dimensional MS on glass slides. Currently, IMS is the only tool that allows for visualization of the binding of fatty acids

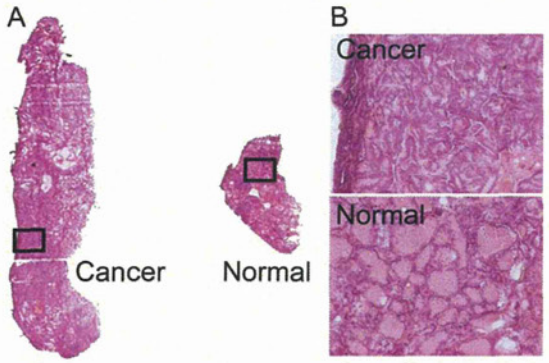

Figure 1. HE-stained section of case 1. (A) Thyroid papillary cancer tissue was localized on the left, and normal thyroid tissue was localized on the right (original magnification 40×). The stromal region was excluded. The ROI was determined from the corresponding HE-staining results. The black boxes indicate the representative region of cancer and normal thyroid tissue. (B) Magnified representative regions of cancer and normal tissue (original magnification 200×). The cancer cells had a high cytoplasmic ratio and displayed nuclear features characteristic of papillary thyroid cancer. Histologic findings of thyroid papillary cancer consisted of columnar thyroidal epithelium set in papillary projection. The normal thyroid tissue is composed of many spherical hollow sacs called thyroid follicles.
doi:10.1371/journal.pone.0048873.g001

to PLs on tissue sections, and this next-generation approach is attracting substantial attention.

The purpose of the present study was to use IMS to elucidate which PL-bound fatty acids were the main components of cell membranes, and in particular, which ones were expressed at relatively high levels in thyroid papillary cancer. This study was the first to investigate cases of PLs in thyroid cancer using IMS analysis, and the first to successfully identify PLs that are highly expressed in thyroid cancer.

Results

1. IMS analysis of case 1

The regions of interest (ROI) in cancer and normal regions were defined according to hematoxylin and eosin (HE)-staining results of a tissue section adjacent to the section used for IMS analysis. Figure 1A provides HE-staining results for case 1 while Figure 1B shows magnified representative regions of cancer and normal tissue. The cancer cells had a high cytoplasmic ratio and displayed nuclear features characteristic of papillary thyroid cancer. Histologic findings of thyroid papillary cancer consisted of columnar thyroidal epithelium set in papillary projection. The normal thyroid tissue is composed of many spherical hollow sacs called thyroid follicles.

Figure 2 shows spectra obtained from case 1 tissue with panels A and B derived from cancer and normal regions, respectively. Both spectrums are average spectrums, and were obtained from ROI in cancer and normal tissue. The number of calculated points in the cancer and normal region was 1425 and 258, respectively. The horizontal axis indicates the mass-to-charge ratio (m/z) and the vertical axis indicates the relative abundance of the ion. The most intense ion is assigned an abundance of 100, and is referred to as the base peak. Most ions formed in a mass spectrometry have a single charge, so that the m/z value is equivalent to the mass itself.

Table 1 shows the top 50 peak picking results for case 1 (excluding isotopic peaks) that were statistically analyzed. Cancer and normal intensity means the average (± standard error) intensity that was divided by the scanning point in cancer and normal regions. Welch t-test was performed between the mean intensity of cancer and normal regions. The m/z values in Table 1 are listed in order of their intensity in the cancer region. The number of the m/z values without isotopic peaks was 40, and the number of the values with significant differences was 26. All m/z values in Table 1 were assigned using the spectrum shown in Figure 2A and B.

2. Visualization of molecular distribution in thyroid tissue of case 1

Figure 3 shows the ion image that was visualized using the m/z values shown in Table 1. The range of each ion color images was optimized manually, so the peaks have different color ranges. In general, malignant cellular proliferation was stimulated due to cell growth factors, which induce an increase in cell density and components of cancer cells such as PLs. Therefore, while the intensity of all m/z values should be higher in cancer regions, the intensity of some values (in particular, m/z 772.5, 782.5 and 848.5) in cancer regions was lower.

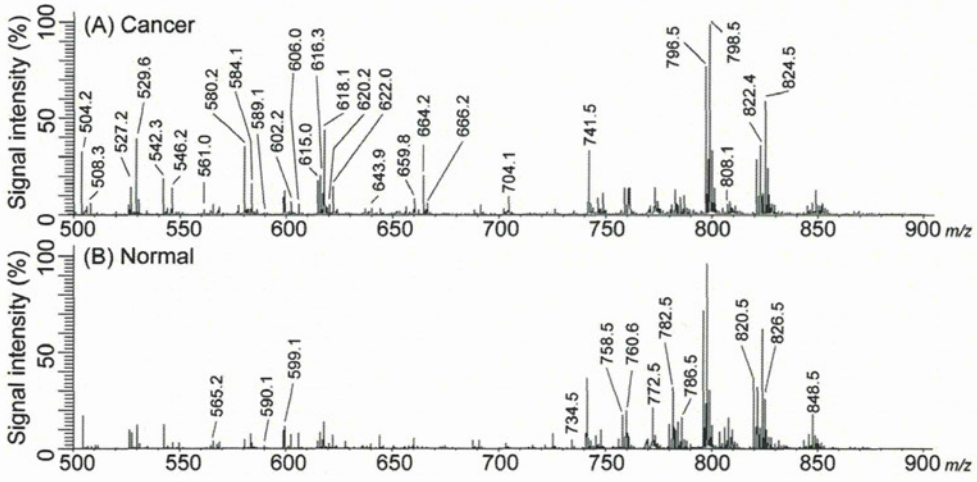

Figure 2. Averaged spectrum for case 1. (A) Spectrum of the cancer region and (B) spectrum of normal region. Each spectrum was averaged from the ROI of cancer and normal tissue in Figure 1. Each number shown in Table 1 was assigned using these spectra.
doi:10.1371/journal.pone.0048873.g002

Table 1. Peak picking and statistical analysis of mass spectra in case 1.

m/z value	Cancer	Normal	P value
798.5	37.1±1.2	28.5±2.6	3.3E-03
824.5	26.7±0.8	26.6±2.4	9.7E-01
796.5	25.1±0.9	17.7±1.7	1.0E-04
618.1	20.4±1.0	5.1±0.6	4.3E-33
529.6	17.0±1.0	3.7±0.4	2.3E-29
580.2	16.2±1.1	2.0±0.3	7.1E-34
822.4	15.9±0.5	13.4±1.3	6.7E-02
504.2	15.6±1.1	6.7±0.8	5.7E-11
741.5	14.0±0.5	11.1±1.0	8.5E-03
664.2	9.5±0.9	0.3±0.1	7.9E-23
616.3	9.0±1.0	4.1±1.7	1.6E-02
826.5	8.7±0.3	8.9±0.9	8.4E-01
820.5	7.8±0.3	9.0±1.1	2.6E-01
584.1	7.4±0.7	1.4±0.2	3.9E-17
622.0	6.7±0.6	1.6±0.3	9.6E-14
760.6	6.5±0.4	7.7±1.0	2.4E-01
758.5	6.3±0.4	7.6±0.9	1.8E-01
527.2	6.2±0.6	3.8±0.5	3.1E-03
782.5	5.5±0.2	12.7±1.3	7.1E-08
542.3	5.5±0.5	0.2±0.0	6.5E-26
772.5	5.4±0.2	12.4±1.9	5.2E-04
615.0	5.4±0.2	1.3±0.1	1.8E-51
848.5	5.0±0.2	8.6±1.0	6.0E-04
546.2	4.8±0.4	0.4±0.1	2.2E-22
786.5	4.6±0.3	7.2±0.9	3.6E-03
704.1	4.0±0.3	0.5±0.1	1.8E-25
599.1	3.9±0.1	3.9±0.3	9.8E-01
659.8	3.7±0.3	1.3±0.2	3.2E-09
666.2	2.7±0.3	0.1±0.0	1.1E-18
508.3	2.6±0.3	0.2±0.0	3.3E-16
606.0	2.5±0.3	1.7±0.3	4.2E-02
808.1	2.5±0.2	2.1±0.7	6.0E-01
602.2	2.3±0.2	1.6±0.3	4.6E-02
565.2	2.0±0.2	2.1±0.3	8.8E-01
643.9	1.3±0.2	1.2±0.2	6.2E-01
734.5	0.7±0.1	3.2±0.7	1.8E-04
561.0	0.7±0.1	0.0±0.0	2.7E-15
620.2	0.3±0.1	0.1±0.0	2.2E-03
590.1	0.2±0.0	0.2±0.0	6.2E-01
589.1	0.1±0.0	0.0±0.0	2.8E-04

doi:10.1371/journal.pone.0048873.t001

3. Comparison of results in all cases

In the same manner as case 1, peak picking and statistical analysis were performed on all cases. Table 2 shows the top 50 peak picking results and excludes isotopic peaks. The m/z values showing no significant differences were excluded. Three m/z values*, including m/z 798.5, 796.5, and 741.5, were found to be common for all cases.

The common m/z values in all cases are displayed in Figure 4. ROIs of cancer and normal tissue in all cases were described in HE-stained results for all cases. The intensity of nearly all m/z values was higher in the cancer region compared to the normal thyroid region. Only the intensity distribution of m/z 741.5 differentiated them from the others.

4. Molecular identification

The three common m/z values in all cases were subjected to tandem mass (MS/MS) analysis to identify the structures of the biomolecules associated with the precursor ions. (Figure 5). The Metabolite MS Search (http://www.hmdb.ca/labm/jsp/mlims/MSDbParent.jsp) was used for referencing.

In MS/MS for PLs with cations, certain characteristic fragment peaks are often detected. The peak at m/z 798.5 (Figure 5A) was identified as phosphatidylcholine (PC) due to the neutral loss of 59 Da and 183 Da during MS/MS, which is indicative of PC [14,15]. Meanwhile, the neutral loss of 256 Da corresponded to palmitic acid. The type of cation adducted to a biomolecule is usually either a sodium or potassium ion, when the sample is obtained from biological tissue. A difference of 38.0 was observed between the m/z 577.5 and 615.5, which is consistent with the replacement of a potassium ion (molecular weight, 39.10) with a proton (molecular weight, 1.01). According to a Metabolite MS search, the peak at m/z 798.5 indicates $[PC\ (16{:}0/18{:}1)+K]^+$. In the same manner, we concluded that m/z 796.5 corresponded to $[PC\ (16{:}0/18{:}2)+K]^+$ (Figure 5B).

The results of m/z 741.5 showed peaks of m/z 682.4 and 558.4 (Figure 5C). The peak at m/z 682.4 corresponded to neutral loss of trimethylamine (59 Da), and the peak at m/z 577.5 corresponded to neutral loss of trimethylamine (59 Da) and cyclophosphate (124 Da). The peak at m/z 184 corresponded to trimethylamine (59 Da), cyclophosphate (124 Da) and a proton ion (1 Da). These results indicated that m/z 741.5 contained an alkali metal adduct phosphocholine; therefore, m/z 741.5 was a PC or sphingomyelin (SM) species. Applying the nitrogen rule to phospholipids, the odd nominal mass indicated SM due to the presence of an additional nitrogen in the sphingosine of SM. We thus concluded that m/z 741.5 was a SM species. The Metabolite MS search indeed suggested that m/z 741.5 corresponded to $[SM\ (d18{:}0/16{:}1)+K]^+$.

Discussion

For more than a century, pathological examinations have been the primary and most important tool for the diagnosis of cancerous regions. Cancer classification itself has been established based on the findings of classical staining methods such as HE staining, and such methods will continue to play a leading role in cancer diagnosis. However, the limitations of classification based on classical staining findings should be noted. It is often the case that patients with the same pathological diagnosis do not always have the same prognosis. Diagnoses are often made based on morphology. Using conventional pathological techniques, we can only conduct morphological observations, and it is difficult to reveal the details of components in tissue sections. *In situ* hybridization and/or immunohistochemistry analyses enable the analysis of the distribution of known molecules; however, it has remained impossible to examine the distribution of unknown molecules. For a detailed and accurate diagnosis, it is necessary to obtain information regarding components such as specific proteins and lipids in a sample.

As an important technique in the proteome generation post-genome era, MS has become widely used in numerous medical fields for the diagnosis and treatment of various diseases, including

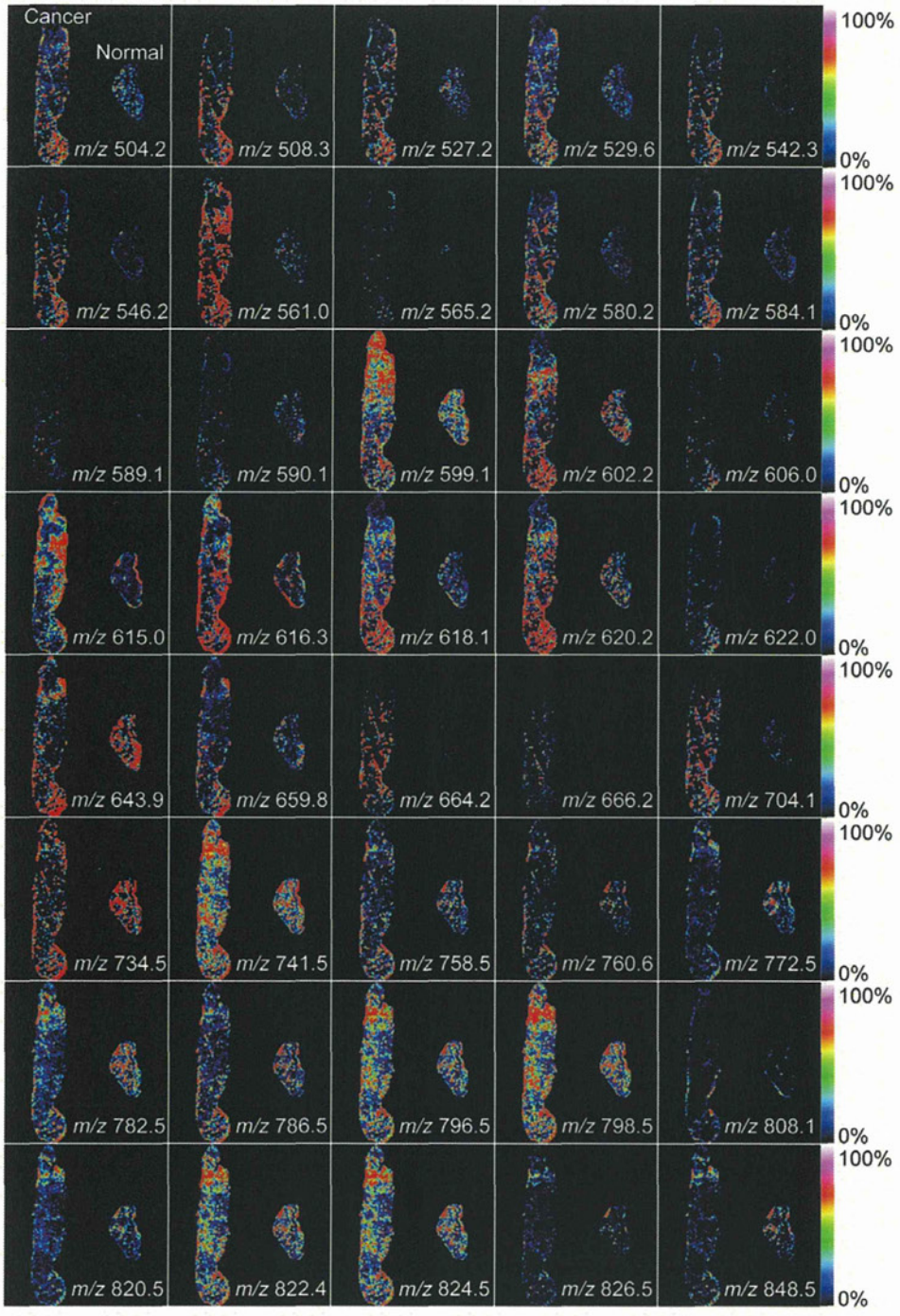

Figure 3. Visualization of molecular distribution in case 1. We visualized ion images corresponding to the results shown in Table 1. In all images, the cancer tissue is on the left and normal tissue is on the right. The distribution of the intensity for each *m/z* value was not constant in the cancer and normal thyroid tissue.
doi:10.1371/journal.pone.0048873.g003

cancer. Numerous novel biomarkers have been identified thus far using MS, which has since been expanded to include IMS [11,16], a technique that enables analysis and visualization of the distribution of individual biomolecules in any area of a tissue section [17]. Thus, this approach is potentially of great significance.

One IMS sequence creates a number of spectrums. To obtain valid information from these spectrums, we performed the addition of an adduct ion. In biological tissue, lipids tend to be positively charged by a proton, sodium, and a potassium ion, which indicates that the distribution of the positive ion influences the distribution of lipids; different values tend to be obtained in the IMS analysis results. In this study, we added potassium salt to the matrix based on reports of Sugiura and co-workers who selectively analyzed PC with different fatty acid compositions by the addition of potassium salt to the matrix solution [18]. When added to the

Table 2. Overview of the *m/z* values that had higher expression levels in cancer regions of all cases.

Case 1	Case 2	Case 3	Case 4	Case 5	Case 6	Case 7
798.5*	798.5*	701.8	798.5*	798.5*	798.7*	798.4*
796.5*	741.5*	676.8	796.5*	741.5*	796.7*	824.4
618.1	796.5*	675.9	820.5	772.5	824.7	796.4*
529.6	824.5	700.8	822.5	796.5*	822.6	822.4
580.2	772.5	704.8	772.5	824.5	826.7	820.4
504.2	760.6	798.5*	741.5*	599.0	820.6	760.5
741.5*	826.6	796.4*	826.5	820.5	748.3	826.5
664.2	822.5	820.4	782.5	782.5	760.8	782.4
584.1	782.5	824.5		822.5	618.2	848.4
622.0	820.5	822.5		583.1	642.2	772.5
527.2	748.2	848.5		826.5	772.6	786.5
542.3	758.5	509.3		848.5	848.7	741.5*
615.0	848.5	741.6*		725.6	782.7	758.4
546.2	786.6	772.4		850.5	741.8*	846.4
704.1	725.6	825.5		756.5	580.3	784.5
659.8	784.6	846.4		748.2	758.7	850.5
666.2	691.3	850.5		844.4	774.3	748.1
508.3	851.6	849.5		846.4	786.8	810.5
561.0	846.4	844.4		760.6	784.7	844.3
620.2	810.5	782.5		780.5	746.4	788.5
589.1	849.5	893.6		808.5	644.1	734.5
	770.5	851.6		810.6	810.7	806.4
	734.6			828.5	504.3	703.5
	850.6			786.6	844.5	770.1
	844.4			758.6	828.6	534.5
	788.6			746.1	806.7	691.1
	534.6				528.3	725.5
	703.6				742.8	
	769.6				691.5	
	853.6				773.6	
	675.4				542.3	
					527.5	
					566.1	
					852.6	
					722.3	
					568.2	
					725.8	

doi:10.1371/journal.pone.0048873.t002

matrix, the potassium salt solution caused a merging of various ion adducts (adducts with proton, sodium, and potassium) into one single potassiated species. This approach enabled us to reduce a number of peaks and made it easier to identify molecules of interest.

In the previous report, we demonstrated the feasibility of IMS as a tool for the analysis of pathological specimens [19]. We showed that IMS can be used to profile biological molecules, including subtypes of PLs. We focused on the distribution of PLs in thyroid papillary cancer. PLs are present as a constituent of the cell membrane and are also expressed in cancer tissue. The intensities of most *m/z* values in cancerous regions are higher than those in normal regions; however, the intensity of some values (*m/z* 772.5, 782.5 and 848.5) in cancer regions was lower than that in normal regions of tissue (see Figure 2 and Table 1). In general, malignant cellular proliferation was stimulated due to cell growth factors, which induce an increase in cell density and components of cancer cells such as PLs. PLs are comprised of numerous combinations of lipids that are based on their length, degree of acyl chain satiation, and the polar head group. Figure 2 suggests that these differences in intensity may arise from the distribution of the thyroid cancer-specific fatty acids that are attached to PLs.

In breast cancer, PLs, especially PCs, in cancer tissues were reported to have a relatively high level of linoleic acid (18:2) and low levels of stearic acid (18:0) [20] and oleic acid (18:1) [21], when compared with normal breast tissue. Luisa *et al.* identified the pattern in the PL pattern and class differences in breast cancer cells [22]. In their report, cancer cells showed a high relative abundance of PC (16:0/18:1) and PC (18:1/18:1) corresponding to $[MH]^+$ at *m/z* 760 and 786. For SM, SM (18:1/16:0) corresponding to $[MH]^+$ at *m/z* 703 was detected mainly in cancer cells.

Another previous report showed that the mRNA of 1-acylglycerol-3-phosphate-O-acyltransferase (AGPAT) 11 that efficiently uses LPA (18:1) as an acyl acceptor and fatty acid 18:1 as an acyl donor is significantly up-regulated in human breast and cervical cancer [23]. Our results show that the *m/z* 798.5 peaks contain fatty acid C18:1, and they are expressed strongly in thyroid cancer regions. While a previous study revealed the selection of specific fatty acid-binding PLs, we provide more information on the relative changes of PLs in thyroid papillary cancer.

In Figure 4, distribution of the intensity in *m/z* 741.5 corresponded to $[SM\ (d18:0/16:1)+K]^+$ and is different from the intensity distribution in the others except for case 1 and 5. HE-staining results showed that the area in which *m/z* 741.5 intensity is expressed strongly mainly consisted of stromal and cancer regions. We reported that the intensity of expressed SM was higher in cancer and stromal regions than in normal regions in a study of colon cancer liver metastasis [19]. Our result was consistent with this report.

Stearoyl-CoA desaturase 1 (Scd1) is the rate limiting enzyme in the cellular synthesis of monounsaturated fatty acids, including C18:1, from saturated fatty acids. Falvella *et al.* reported that Scd1 gene overexpression is associated with hepatocarcinogenesis in mice [24]. Scaglia *et al.* reported that inhibition of Scd1 expression in human lung cancer cells impairs tumorigenesis, whereas the rate of apoptosis was elevated [25]. These reports indicate that Scd1 causes an increase in C18:1 in cancer tissue.

The type of fatty acid influences cell shape and cell membrane fluidity [9]. The alterations of cancer cell membrane fluidity may influence the biological behavior of cancer such as invasion/metastasis. IMS is the only tool that allows for the visualization of the binding of fatty acids to PLs on tissue sections. Recently, an increasing number of reports has focused on the relationship between pathological insults and PLs, including PCs [26], i.e., the remodeling pathway of PLs [27]. It is expected that IMS analysis will help to achieve a better understanding of the relationship between fatty acids and cancer mechanisms.

Using IMS, we directly profiled PC and SM expression from tissue samples. This explorative profiling of PL on the basis of IMS analysis provided results that emphasize the potential of IMS for pathological diagnoses. The potential application of IMS analysis in the clinical workflow has been suggested in a previous report [28]. Compared to conventional methods such as MS and immunohistochemistry, IMS has certain advantages as a clinical

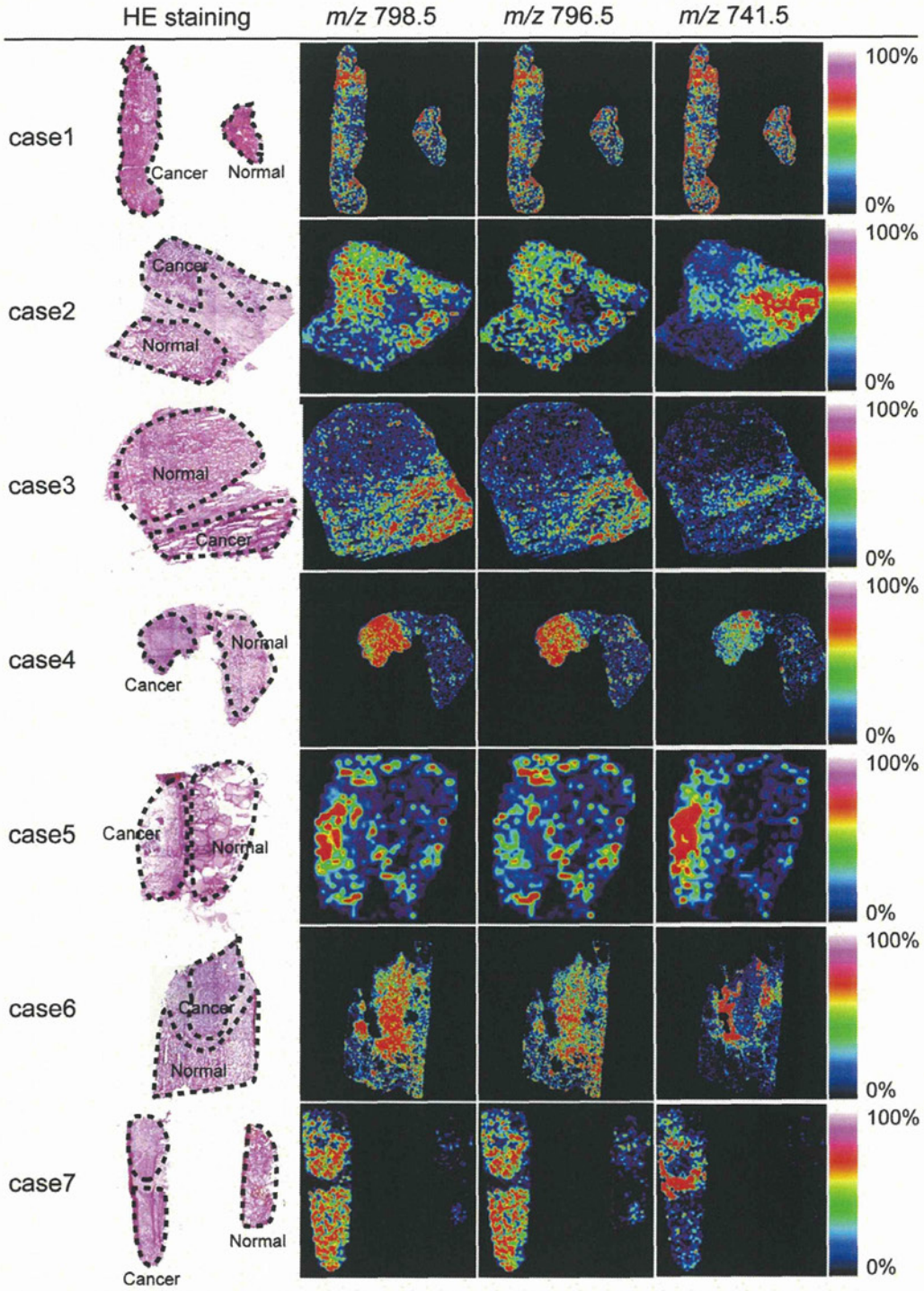

Figure 4. Visualization of molecular distribution of *m/z* values that were expressed to higher levels in cancer tissue from all cases. The ROI of each case is defined by a dashed line in HE-staining images. The intensity of all values in the cancer region was higher than in normal regions. The distribution of intensity in *m/z* 741.5 was different from the distribution of intensity in the other *m/z* values.
doi:10.1371/journal.pone.0048873.g004

application. Sample purification and extraction is necessary prior to MS analysis. In addition, the performance of an antibody-based assay in immunohistochemistry is always degraded to easily observed changes in intensity or localization. On the other hand, IMS analysis requires only a simple pretreatment, i.e., matrix deposition and fixing the IMS condition settings. This means that time is not lost between sample collection and analysis. It is predicted that IMS will be readily introduced into the pathological examination setting.

Recent studies have provided evidence of the clinical benefits of IMS analysis, namely, that its profiles discriminate between other diseases and prostate cancer [29] and the HER2 status of breast cancer [30]. In these reports, IMS enabled the classification of morphological and diagnostic features. A recently developed

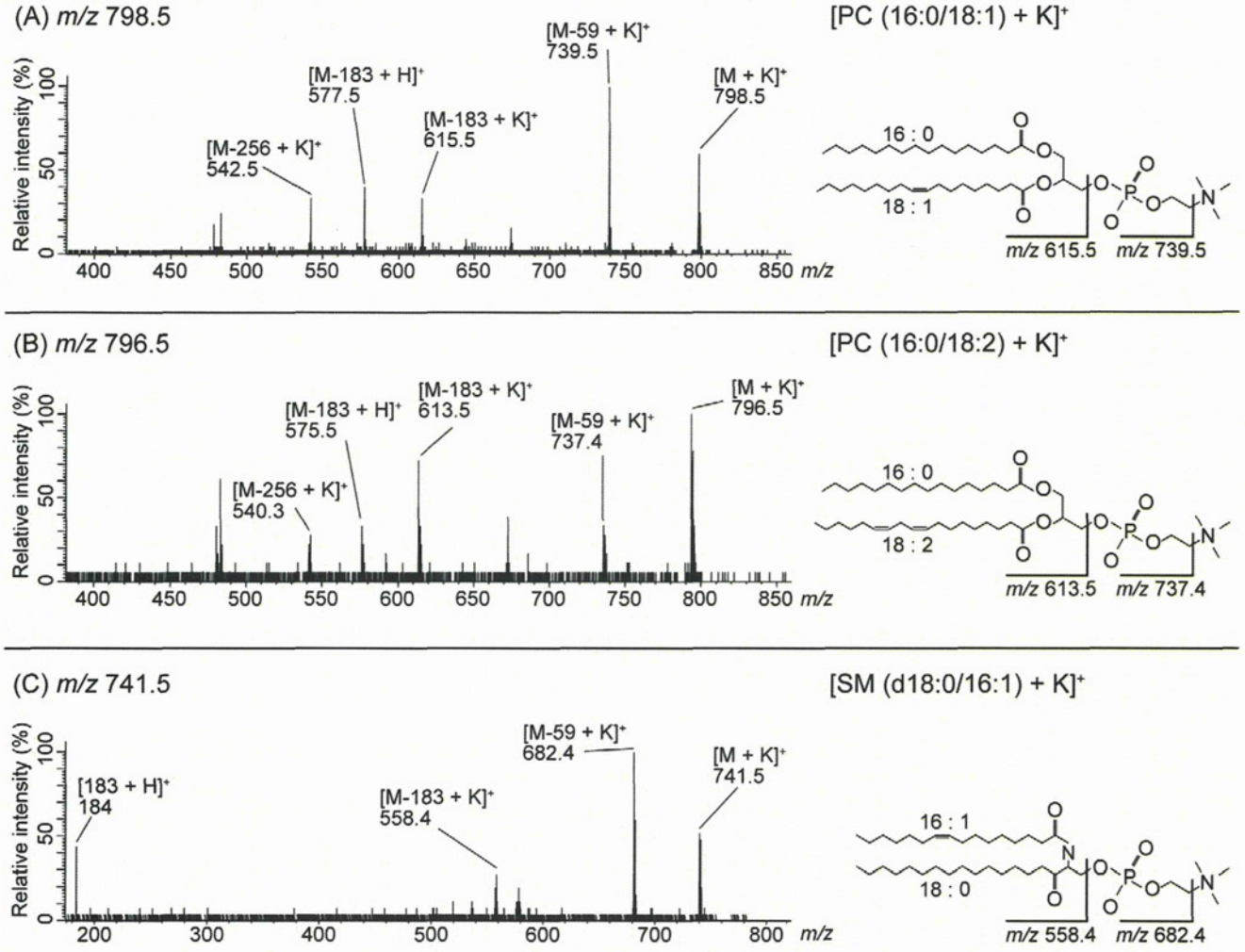

Figure 5. Identified molecules. (A) MS/MS data of *m/z* 798.5. The structure of one peak was analyzed. The product ion spectrum of *m/z* 798.5 as a precursor ion was obtained by MS/MS of thyroid papillary cancer region. This biomolecule was identified by neutral loss as [PC (16:0/18:1)+K]$^+$. In the same manner, in (B) *m/z* 796.5 was identified as [PC (16:0/18:2)+K]$^+$. (C) *m/z* 741.5 was identified as [SM (d18:0/16:1)+K]$^+$.
doi:10.1371/journal.pone.0048873.g005

variant of IMS analysis, referred to as "targeted imaging mass spectrometry" (TIMS), was described by Thiery and colleagues [31]. Such targeted analysis enabled the visualization of molecules of interest directly from the tissue section by the use of laser reactive photocleavable molecular tags attached to antibodies. This approach provides quantification by estimating the signal intensity, and an excellent signal-to-noise ratio in the resulting spectrums. It is important to note that this diagnosis was made on a single sample section; few cancer biopsies were available, and more would be needed to quantitate a biomarker by IHC. In the future, IMS analysis will provide new biomarkers and in turn, new pathological categories, and could therefore become a critical diagnostic tool in the clinical setting.

Materials and Methods

Ethics statement

Sample collection and archiving of patient data was performed using written informed consent, and was approved by the ethical committee of Kyoto University. This study was performed in accordance with the Kyoto University guidelines for pathological specimen handling.

1. Sample preparation

Seven Japanese patients who underwent routine thyroidectomy at Kyoto University Hospital were involved in the present study. Six women and one man were included and the average patient age was 52 years. There was no recurrence in all cases. Samples were obtained from a thyroid cancer section and adjacent normal tissue immediately after tumor resection. The pathological diagnosis was papillary thyroid carcinoma. The obtained tissue was frozen in liquid nitrogen immediately to minimize degradation and was kept at −80°C. The tissue sections were sliced to a thickness of 10 μm using a Cryostat (CM 1950; Leica, Wetzler, Germany). One section was mounted onto an indium-tin-oxide-coated (ITO) glass slide for IMS analysis. Another section adjacent to that used for IMS was mounted onto a glass slide (MAS coat; Matsunami, Osaka, Japan) for HE staining to identify cancer and normal thyroid regions.

2. Matrix deposition

The matrix solution was prepared by dissolving 50 mg 2, 5-dihydroxybenzoic acid (DHB; Bruker Daltonics, Leipzig, Germany) in 1 mL 70% methanol and 10 mM potassium acetate. DHB is a widely used matrix for low molecular weight molecules.

The addition of potassium salt to the matrix solution caused a merging of various ion adducts into one single potassiated species. This approach enabled us to reduce the number of peaks and simplified the identification of molecules of interest. A thin matrix layer was applied to the surface of the tissue sections using a 0.2-mm nozzle airbrush (Procon Boy FWA Platinum; Mr. Hobby, Tokyo, Japan) maintained at 15 cm from the tissue surface. The total amount of matrix solution on each slide was 1 mL. The spraying technique enabled full matrix coverage over the entire tissue surface and facilitated the co-crystallization of the matrix and bio-molecules.

3. Imaging mass spectrometry analysis

The tissue sections were analyzed using a matrix-assisted laser desorption/ionization-time-of-flight/time-of-flight (MALDI-TOF/TOF)-type instrument, Ultraflex II TOF/TOF (Bruker Daltonics), which was equipped with a 355-nm Nd: YAG laser at 200 Hz repetition. Data were acquired in the positive-ion mode using an external calibration method with ions from DHB, angiotensin II and bradykinin. Their decomposition products covered from m/z 100 to 1200. Calibration proteins were deposited on the surfaces of sample materials. Each raster scan was automatically performed in the regions of cancer and normal tissue. The interval between data points was 100-μm, and 100 laser beam shots were irradiated on each data point. The mass spectrometry parameters were optimized manually to obtain the highest sensitivity with m/z values in the range of 400–900. All spectra were acquired automatically using flexImaging 2.1 software (Bruker Daltonics), and the file format was converted to enable analysis with Biomap (http://www.maldi-msi.org) and SIMtools software (in-house software; Shimadzu Corporation). The ion image was visualized using Biomap software.

4. Comparison of signal intensities between cancer and normal thyroid regions

IMS analysis results were integrated, and the ROI in cancer and normal thyroid tissues were defined corresponding to HE results using SIMtools software. The top 50 peaks excluding isotopic peaks were picked from ROI that was defined as cancer and normal thyroid region, and the statistical difference was determined by Welch t-test. Differences with $p<0.01$ were considered significant.

5. Comparison of results for all cases

We performed IMS and statistical analysis on all cases, and picked the m/z value that had significantly higher expression in cancer regions and was common in all cases.

6. Molecular identification

The common m/z values in all cases were employed for MS/MS analysis for molecule identification. MS/MS analysis was performed on tissue sections in the positive-ion mode using QSTAR Elite (Applied Biosystems/MDS Sciex, Foster City, CA, USA), a hybrid quadrupole/TOF mass spectrometer equipped with an orthogonal MALDI source and a pulsed Nd: YAG laser. Metabolite MS Search was used to determine the molecular species of PLs. The matrix solution was prepared in the same way as for IMS analysis. The mass spectrometry parameters were optimized manually to obtain the highest sensitivity with m/z values in the range of 100–850.

Author Contributions

Conceived and designed the experiments: SI IT TH SH MK MS. Performed the experiments: SI TH YT. Analyzed the data: SI IT TH NM MS. Contributed reagents/materials/analysis tools: SI IT SH JI TH NM YT MS. Wrote the paper: SI IT TH NM SH JI. Sample collection: SI IT SO TK YK MK SH JI.

References

1. Sipos J, Mazzaferri E (2010) Thyroid cancer epidemiology and prognostic variables. Clin Oncol (R Coll Radiol) 22: 395–404.
2. Bojunga J, Zeuzem S (2004) Molecular detection of thyroid cancer: an update. Clin Endocrinol (Oxf) 61: 523–530.
3. Carpi A, Mechanick J, Saussez S, Nicolini A (2010) Thyroid tumor marker genomics and proteomics: diagnostic and clinical implications. J Cell Physiol 224: 612–619.
4. Brown L, Helmke S, Hunsucker S, Netea-Maier R, Chiang S, et al. (2006) Quantitative and qualitative differences in protein expression between papillary thyroid carcinoma and normal thyroid tissue. Mol Carcinog 45: 613–626.
5. Netea-Maier R, Hunsucker S, Hoevenaars B, Helmke S, Slootweg P, et al. (2008) Discovery and validation of protein abundance differences between follicular thyroid neoplasms. Cancer Res 68: 1572–1580.
6. Mann E, Spiro J, Chen L, Kreutzer D (1994) Phospholipid metabolite expression by head and neck squamous cell carcinoma. Arch Otolaryngol Head Neck Surg 120: 763–769.
7. Gschwind A, Prenzel N, Ullrich A (2002) Lysophosphatidic acid-induced squamous cell carcinoma cell proliferation and motility involves epidermal growth factor receptor signal transactivation. Cancer Res 62: 6329–6336.
8. Coussens L, Werb Z (2002) Inflammation and cancer. Nature 420: 860–867.
9. Cullis PR, Fenke DB, Hope MJ (1996) Biochemistry of Lipids, Lipoproteins and Membranes.
10. Stubbs CD, Smith AD (1984) The modification of mammalian membrane polyunsaturated fatty acid composition in relation to membrane fluidity and function. Biochim Biophys Acta 779: 89–137.
11. Stoeckli M, Chaurand P, Hallahan D, Caprioli R (2001) Imaging mass spectrometry: a new technology for the analysis of protein expression in mammalian tissues. Nat Med 7: 493–496.
12. Shimma S, Sugiura Y, Hayasaka T, Zaima N, Matsumoto M, et al. (2008) Mass imaging and identification of biomolecules with MALDI-QIT-TOF-based system. Anal Chem 80: 878–885.
13. Stoeckli M, Farmer TB, Caprioli RM (1999) Automated mass spectrometry imaging with a matrix-assisted laser desorption ionization time-of-flight instrument. J Am Soc Mass Spectrom 10: 67–71.
14. Al-Saad K, Siems W, Hill H, Zabrouskov V, Knowles N (2003) Structural analysis of phosphatidylcholines by post-source decay matrix-assisted laser desorption/ionization time-of-flight mass spectrometry. J Am Soc Mass Spectrom 14: 373–382.
15. Hayasaka T, Goto-Inoue N, Sugiura Y, Zaima N, Nakanishi H, et al. (2008) Matrix-assisted laser desorption/ionization quadrupole ion trap time-of-flight (MALDI-QIT-TOF)-based imaging mass spectrometry reveals a layered distribution of phospholipid molecular species in the mouse retina. Rapid Commun Mass Spectrom 22: 3415–3426.
16. Caprioli R, Farmer T, Gile J (1997) Molecular imaging of biological samples: localization of peptides and proteins using MALDI-TOF MS. Anal Chem 69: 4751–4760.
17. Enomoto H, Sugiura Y, Setou M, Zaima N (2011) Visualization of phosphatidylcholine, lysophosphatidylcholine and sphingomyelin in mouse tongue body by matrix-assisted laser desorption/ionization imaging mass spectrometry. Anal Bioanal Chem 400: 1913–1921.
18. Sugiura Y, Setou M (2009) Selective imaging of positively charged polar and nonpolar lipids by optimizing matrix solution composition. Rapid Commun Mass Spectrom 23: 3269–3278.
19. Shimma S, Sugiura Y, Hayasaka T, Hoshikawa Y, Noda T, et al. (2007) MALDI-based imaging mass spectrometry revealed abnormal distribution of phospholipids in colon cancer liver metastasis. J Chromatogr B Analyt Technol Biomed Life Sci 855: 98–103.
20. Williams CM, Maunder K (1993) Fatty acid compositions of inositol and choline phospholipids of breast tumours and normal breast tissue. European journal of clinical nutrition 47: 260–267.
21. Chajes V, Niyongabo T, Lanson M, Fignon A, Couet C, et al. (1992) Fatty-acid composition of breast and iliac adipose tissue in breast-cancer patients. International journal of cancer Journal international du cancer 50: 405–408.
22. Doria ML, Cotrim Z, Macedo B, Simoes C, Domingues P, et al. (2011) Lipidomic approach to identify patterns in phospholipid profiles and define class differences in mammary epithelial and breast cancer cells. Breast Cancer Research and Treatment: 1–14.

23. Agarwal A, Garg A (2010) Enzymatic activity of the human 1-acylglycerol-3-phosphate-O-acyltransferase isoform 11: upregulated in breast and cervical cancers. J Lipid Res 51: 2143–2152.
24. Falvella FS, Pascale RM, Gariboldi M, Manenti G, De Miglio MR, et al. (2002) Stearoyl-CoA desaturase 1 (Scd1) gene overexpression is associated with genetic predisposition to hepatocarcinogenesis in mice and rats. Carcinogenesis 23: 1933–1936.
25. Scaglia N, Igal RA (2008) Inhibition of Stearoyl-CoA Desaturase 1 expression in human lung adenocarcinoma cells impairs tumorigenesis. International journal of oncology 33: 839–850.
26. Linkous A, Yazlovitskaya E (2010) Cytosolic phospholipase A2 as a mediator of disease pathogenesis. Cell Microbiol.
27. Shindou H, Hishikawa D, Harayama T, Yuki K, Shimizu T (2009) Recent progress on acyl CoA: lysophospholipid acyltransferase research. J Lipid Res 50 Suppl: S46–51.
28. Cazares LH, Troyer DA, Wang B, Drake RR, John Semmes O (2011) MALDI tissue imaging: from biomarker discovery to clinical applications. Anal Bioanal Chem 401: 17–27.
29. Schwamborn K, Krieg RC, Reska M, Jakse G, Knuechel R, et al. (2007) Identifying prostate carcinoma by MALDI-Imaging. Int J Mol Med 20: 155–159.
30. Rauser S, Marquardt C, Balluff B, Deininger SO, Albers C, et al. (2010) Classification of HER2 receptor status in breast cancer tissues by MALDI imaging mass spectrometry. J Proteome Res 9: 1854–1863.
31. Thiery G, Shchepinov MS, Southern EM, Audebourg A, Audard V, et al. (2007) Multiplex target protein imaging in tissue sections by mass spectrometry–TAMSIM. Rapid Commun Mass Spectrom 21: 823–829.

Anal Bioanal Chem (2012) 403:1775–1776
DOI 10.1007/s00216-012-5922-x

EDITORIAL

Biomedical mass spectrometry

Toyofumi Nakanishi · Mitsutoshi Setou · Tomiko Kuhara

Published online: 10 April 2012

The 36th Annual Meeting of the Japanese Society for Biomedical Mass Spectrometry (JSBMS) was held on September 15 and 16, 2011, in the Galaxy Hole Room in Hotel Hankyu Expo Park, Osaka, Japan. The theme of the meeting was "New challenges not for clinical research but for medical services: from mass profiling to mass imaging " and covered a variety of biomedical applications, such as diagnosis and disease state assessment of inherited metabolic disorders, forensic toxicological analysis, proteomics, metabolomics, and imaging mass spectrometry. At this meeting, we partially collaborated with the Japan Society of Mass Spectrometry (JSMS) during the invited sessions on the first day.

On the first day, there was joint program with the JSMS in the afternoon session. We invited four famous researchers: Prof. Shu-ichi Ikeda from Shinshu University (School of Medicine)—he presented a lecture entitled "Pathogenesis and therapeutic approaches in systemic amyloidosis"; Dr. Pierre Chaurand from Montreal University (Department of Chemistry)—he presented a lecture entitled "Imaging mass spectrometry: current performances and upcoming

Published in the special paper collection *Biomedical Mass Spectrometry* with guest editors Toyofumi Nakanishi and Mitsutoshi Setou.

T. Nakanishi (✉)
Clinical and Laboratory Medicine, Osaka Medical College,
2-7 Daigaku-cho,
Takatsuki, Osaka 569-8686, Japan
e-mail: nakanisi@poh.osaka-med.ac.jp

M. Setou
Department of Cell Biology and Anatomy,
Hamamatsu University School of Medicine,
1-20-1 Handayama,
Hamamatsu, Shizuoka 431-3192, Japan

T. Kuhara
Division of Human Genetics, Medical Research Institute,
Kanazawa Medical University,
Uchinada-machi,
Kahoku-gun, Ishikawa 920-0293, Japan

Toyofumi Nakanishi is an associate professor of clinical and laboratory medicine at Osaka Medical College. His research interests include clinical application of imaging mass spectrometry and clinical diagnosis of soft-ionization mass spectrometry coupled with immunoprecipitation. He is the author of 65 peer-reviewed papers, 35 scientific papers, and 13 book chapters.

Mitsutoshi Setou has been a full professor of anatomy and cell biology at the Hamamatsu University School of Medicine since 2008. His research interests include development and application of imaging mass spectrometry and systems biology with "omics" technologies. He is the author of over 100 peer-reviewed papers, 150 scientific papers, and ten book chapters, and is the editor of a book on imaging mass spectrometry.

Tomiko Kuhara, president of JSBMS from 2007 to 2011, is a professor of human genetics at Kanazawa Medical University. Her research interests have included the development and application of metabolic profiling based on gas chromatography/mass spectrometry since the 1970s and metabolomic profiling since the early 1990s. The diagnostic procedures she has developed are extremely useful for noninvasive differential chemical diagnosis of around 130 disease conditions (including more than 100 inherited metabolic disorders) and for personalized medicine. The procedures are also very effective for all stages of drug R & D.

challenges"; Dr. Yoshinao Wada, General Director of the Osaka Prefectural Research Institute for Maternal and Child Health—he presented a lecture entitled "Past and future trends of biomedical applications: measuring quality or quantity"; and Prof. Frantisek Turecek from Washington University (Department of Chemistry)—he presented a lecture entitled "Tandem mass spectrometry and clinical enzymology: toward newborn screening of lysosomal storage disorders." Also, on the same day, three young scientists (Dr. Daisuke Saegusa from Tohoku University, Dr. Ikuko Yao from Kansai Medical University, and Dr. Mototada Hichiri from the National Institute of AIST) won the awards for the best poster presentations. There was a symposium on forensic and toxicological mass spectrometry, organized by Dr. Hitoshi Tsuchihashi from Osaka Medical College. In this session, a surprise guest presented a lecture entitled "Drug history in a longitudinally sliced hair section by MALDI imaging." The group concerned were the first to demonstrate the traceability of drug history every few hours using only a sliced hair section (*J. Mass Spectrom.* 46:411-416, 2011).

On the second day, there were two symposia, entitled "New applications to clinical microbiology by mass spectrometry," organized by Prof. Fumio Nomura from Chiba University, and "Developments of imaging mass spectrometry," organized by Prof. Mitsutoshi Setou from Hamamatsu Medical University. In workshops I and II, there were technical sessions. One was entitled "Current MS technology and its associate techniques," organized by Prof. Shigeo Ikegawa from Kinki University and Prof. Kuniaki Saito from Kyoto University. The other was entitled "Applications of MS techniques: questions and answers for good-quality MS data," organized by Dr. Takeshi Kasama from Tokyo Medical and Dental University and Toshie Takahashi from Tokyo University.

This special issue is based on the presentations at the 36th Annual Meeting of JSBMS in Osaka Senri. There were 23 oral presentations (three regular sessions, three symposia, and four invited lectures), 36 poster presentations, and 202 participants at this meeting (see Fig. 1). We would like to thank all speakers, presenters, participants, and staff members for the excellent papers, earnest discussion, and cooperation at this fruitful meeting.

Fig. 1 Participants of the 36th Annual Meeting of the Japanese Society for Biomedical Mass Spectrometry in Osaka Senri

Current Topics

Challenge of Mass Spectrometry toward the Elucidation of Life Phenomena

Development of Imaging Mass Spectrometry

Yusuke Saito, Michihiko Waki, Saira Hameed, Takahiro Hayasaka, and Mitsutoshi Setou*

Department of Cell Biology and Anatomy, Hamamatsu University School of Medicine; 1–20–1 Handayama, Higashi-ku, Hamamatsu, Shizuoka 431–3192, Japan.

Received February 3, 2012

We have developed a mass microscope in which a microscope is combined with high-resolution matrix assisted laser desorption/ionization-imaging mass spectrometry (MALDI-IMS). This technique is a powerful tool for investigating the spatial distribution of biomolecules without the need for any time-consuming extraction, purification, and labeling procedures for biological tissue sections. The mass microscope provides clear images with regards to the distribution of hundreds of biomolecules in a single measurement, and also helps in determining the cellular profile of the biological system. In this review, we focus on some of the recent developments in clinical applications and describe how the mass microscope can be employed to assess pathomorphology and pharmacokinetics.

Key words imaging; mass spectrometry; microscopy; analytical biochemistry; drug kinetics

1. INTRODUCTION

Imaging is a technique that can be used to visualize cellular and molecular processes that occur in living organisms in a two-dimensional (2-D) or three-dimensional (3-D) fashion, without perturbing the structure of the system. The various techniques currently available include X-rays,[1] nuclear magnetic resonance,[2] cryo-electron microscopes,[3] positron emission tomography,[4] immunohistochemistry,[5–8] green fluorescent protein labeling,[9–12] and luciferase.[13] The green fluorescent protein labeling technique involves over expression of the fusion protein of the concerned molecule and green fluorescent protein.[12,14] However, these techniques can only provide information on the structure of the material. There is also a "nonlabeling" technique even at the electron microscopic level,[3] and yet there is still a serious limitation on the object preference. Imaging mass spectrometry (IMS)[15] is an emerging technique that is expected to at once resolve these problems in conventional morphological examinations. In IMS, mass spectra associated with spatial information can be simultaneously recorded to obtain expression patterns of various molecules in specimens to be analyzed. This new generation of mass spectrometry (MS) has been used for the analysis of biological compounds at either the tissue[16–19] or single-cell level.[20–23] Recent IMS studies have been conducted on a variety of topics, including biological applications[24–30] and pathological applications.[31,32] In addition to the analysis of protein described in the above references, direct lipid analysis in mammalian tissues[33,34] has also been conducted, and histopathological materials[35] and pharmacokinetics in rat whole body sections[36] have been studied.

IMS can be used to visualize the spatial distribution of biomolecules based on the mass-to-charge ratio (m/z) of the target molecule in the mass spectrum. Several ionization methods, such as desorption electrospray ionization (DESI),[37] secondary ion mass spectrometry (SIMS),[38] and matrix-assisted laser desorption/ionization (MALDI) have been investigated.[39] DESI is an ionization technique by which the molecules are ionized without addition of organic matrix under ambient conditions. In this method, the surface of the sample is analyzed by charged droplets of solvent, generated during the electrospraying. DESI has a limited spatial resolution of 0.3–0.5 mm, which is not a sufficiently high resolution for imaging. SIMS on the ion microprobe offers the best combination of spatial resolution (20 μm beam diameter) and precision (0.2 per mL for sulfur isotopes). This technique is applicable for the analysis of small molecules (<1 kDa) because the high energy of the SIMS causes the fragmentation of larger molecules. On the other hand, MALDI is used to visualize biomolecules such as lipids less than 1 kDa as well as peptides and proteins over 10 kDa.

MALDI-IMS is a powerful tool that allows the simultaneous mapping of hundreds of molecules in a tissue section in a single measurement. To use a mass spectrometer as an imaging instrument, it is essential for the spectrometer to be equipped with an automatic rastering function, automatic data acquisition system, and visualization software. Recently, several manufacturers have released novel instruments having these features. Almost all manufacturers have developed in-house software for their instruments and have included a driver for instrument and image reconstruction. On the other hand, the user-friendly visualization software BioMap[40] is freely available; it is used commonly in mass imaging (MALDI MSI HP, http://www.maldi-msi.org/content).

Our group has developed the original equipment in collaboration with Shimadzu Corporation of Japan and extended the techniques for molecular profiling of different tissue samples, such as brain,[41–43] liver,[44] testis,[45] and retina[46] of mice, and colon cancer in human,[47] involving sample preparation,[25,48–50] and the nanoparticle-based ionization process in IMS.[51–53] In

* To whom correspondence should be addressed. e-mail: setou@hama-med.ac.jp